Journal of Cerebral Blood Flow & Metabolism (2013) 33, 669–672

www.jcbfm.com

BRIEF COMMUNICATION

On the normalization of cerebral blood flow

Romain Guibert[1,2,3,4], Caroline Fonta[3,4], François Estève[5,6] and Franck Plouraboué[1,2]

Cerebral blood flow (CBF) is the most common parameter for the quantification of brain's function. Literature data indicate a widespread dispersion of values that might be related to some differences in the measurement conditions that are not properly taken into account in CBF evaluation. Using recent high-resolution imaging of the complete cortical microvasculature of primate brain, we perform extensive numerical evaluation of the cerebral perfusion. We show that blood perfusion associated with intravascular tracers should be normalized by the surface of the voxel rather than by its volume and we consistently test this result on the available literature data.

Journal of Cerebral Blood Flow & Metabolism (2013) **33,** 669–672; doi:10.1038/jcbfm.2013.39; published online 13 March 2013

Keywords: brain imaging; brain perfusion; computed tomography; hemodynamics; microcirculation

INTRODUCTION

Cerebral blood flow (CBF) is a key parameter for quantifying normal, altered, or pathologic brain functioning, both in medical current practice and in cognitive neuroimaging studies. Relative comparison of this parameter is generally used for the purpose of identifying a given effect after a treatment or a condition change at the individual level.[1] Nevertheless, there is also a great interest in providing consistent perfusion estimation which, with different methods, differs by a fair amount.[2–4] As stated by Kudo *et al*,[4] little is known about the relationship between CBF measured with different methods. The CBF estimations with computed tomography perfusion (CT perfusion), positron emission tomography (PET), or single-photon emission computed tomography are thus very difficult to compare, even if correcting for large vessel over-contribution in CT perfusion leads to more consistent results.[4] Such comparison is difficult for two reasons. First at the fundamental level, the highly complex vascular hemodynamic events leading to brain perfusion are poorly known. Second, the precise relationship between hemodynamics and the signals recorded with CT perfusion, positron emission tomography, or single-photon emission computed tomography are also poorly understood from a quantitative viewpoint. Hence, at the level of each individual technique, the comparison between different operating modes is crucial for considering absolute CBF. Among those techniques, CT perfusion built on a direct and robust relationship between signal and contrast agent perfusion techniques is generally considered to report the most reliable CBF values.[3–5] But for all those methods, a current convention states that part of the methodological variability can be rescaled into a volume normalization (generally expressed in 100 ml volume or in 100 g tissue weight). Recent investigations have nevertheless challenged the CBF normalization by voxel volume and suggest an alternative scaling.[6] More precisely, based on allometric arguments associated with brain capillary length, diameter, and neuron density scalings, Karbowski[6] rather proposes to normalize the brain perfusion by the one-sixth power of the considered voxel volume V.

In this contribution, we challenged intrinsic CBF pixel size-independent normalization with a new standpoint. We analyzed, at the fundamental level, the blood perfusion inside the cerebral cortex starting from an exhaustive description of its vessel network from pia surface down to capillary scale inside gray matter. We specifically focus on the contribution of intravascular blood flow to cerebral perfusion.

MATERIALS AND METHODS

Synchrotron microtomography[7] has been used to image Barium particles in solution injected in primate brain microvascular networks with a 1.4^3 μm^3/voxel resolution. The animal (5-year-old male marmoset *Callithrix jacchus*) was from the in-house colony at the accredited primate center of the Center de Recherche Cerveau et Cognition (CNRS/ Univertité de Toulouse, France, n°B.31.555-01). The experimental procedures were performed in accordance with the recommendations of the EEC and the French Regional committee for the use of laboratory animals (authorization number MP/07//3810/09). The high concentration of the Barium contrast agent allows a precise identification of vessels from the reconstructed gray-scale three-dimensional images. Traditional image processing method[8] (hysteresis thresholding, morphologic mathematical opening/closure procedures) permits to segment the vessel structure without loss of information. The vessels are then digitalized using a skeletonization procedure[8] so that the vessel shapes and the microvascular network topology of the entire network can be reconstructed at the micron scale. It is important to mention that an additional gap-filling procedure[9] is also added in the image postprocessing step to compensate for the imperfect contrast agent injection inside some capillaries. This compensation might not be perfect, but the remaining unconnected capillaries are drastically reduced by this procedure. The efficiency of reconnections might also be increased by a proper use of gap distance and directional parameters to be defined for permitting reconnection. None of the following results are affected by those post treatments since their robustness relies on the fact that the number of capillaries crossing each face of the considered voxel is large (i.e., larger than 30 for averaging concepts being meaningful), which might even be larger in the case of missing connections.

The blood perfusion inside this highly complex network is then computed with a network method[10] that permits the evaluation of the blood pressure and flux inside each individual vessel segment. Finally,

[1]Institut de Mécanique des Fluides de Toulouse, Université de Toulouse, INPT, UPS, IMFT, Toulouse, France; [2]CNRS, IMFT, Toulouse, France; [3]Centre de Recherche Cerveau et Cognition, Université de Toulouse, UPS, Toulouse, France; [4]CNRS, CerCo, Toulouse, France; [5]Grenoble Institut de Neurosciences, INSERM U836 Grenoble Cedex 9, France and [6]ID17 Medical Beamline, European Synchrotron Radiation Facility, Grenoble Cedex 9, France. Correspondence: Dr F Plouraboué, Institut de Mécanique des Fluides de Toulouse, Allée Camille Soula, Toulouse 31400, France.
E-mail: franck.plouraboue@imft.fr
This study was supported by a PhD grant from Paul Sabatier Toulouse 3 University to RG and funding (AO3) from the Scientific Board of Paul Sabatier Toulouse 3.
Received 21 June 2012; revised 25 January 2013; accepted 27 January 2013; published online 13 March 2013

the statistical analysis of the data discussed in the following sections uses classic Student's *t*-test.

RESULTS

Figure 1A illustrates the largest cube of 8 mm^3 that could be extracted from the complete reconstruction of a cylindrical sample of primate cortex excluding the pia matter (Figure 1B), which is essential for applying relevant boundary conditions.[10] The resulting prediction for the blood pressure and flow distribution depends on the considered blood rheological model; we already analyzed this issue in a recent study.[10] Here, we show that the CBF measurement depends on the size of the processed virtual voxel, i.e., the size of the cubic box. From evaluating CBF using different voxel sizes, we have been able to analyze its size dependence. The total blood perfusion flux Q in a given voxel is directly evaluated from summing the input contributions of all the vascular segments that are also equal to the output ones since blood is incompressible. It obviously increases when sampling more and more vessels so that it is significantly different when varying the voxel-box size ($P<5\times10^{-3}$ in Student's *t*-tests of Figure 2A). The size sampling is obtained by dividing the initial voxel (box) by two in each direction. From the initial 8 mm^3 cube we then get 8, 64, and 512 voxels (whose respective cube edge is 1000, 500, and 250 microns) of respectively 1, 0.125, and 0.015 mm^3. The perfusion per volume unit (equivalent to CBF) is then computed in each voxel. A volumetric size dependence of the CBF would have suggested a slope equal to three for perfusion Q variation with the voxel dimension in each direction in the bilogarithmic representation of Figure 2A (the average value of Q and its root mean square variations are represented). Nevertheless, the observed slope is very close to two, as indicated with dotted lines (Figure 2A). We then tested the usual volumetric CBF rescaling in Figure 2B and consistently found that it is indeed significantly voxel size dependent, as indicated by Student's *t*-tests ($P<10^{-3}$). On the contrary, when rescaling the perfusion flux Q by the voxel surface S, its evaluation at different scales does not statistically differ anymore (Student's *t*-tests $P>0.75$ in Figure 2C). Albeit presented here for one *in vivo* blood rheology model,[11] this finding is robust to any rheology models previously analyzed[10] so that this observation is a very strong property of blood perfusion spatial distribution. We also statistically tested the $Q/V^{1/6}$ normalization[6] and found that it does not provide a scale-invariant quantity for the four different voxel sizes chosen. This observation highly suggests that the usual normalization for CBF is not voxel independent, the implication of which is considerable for comparison with future studies for which spatial resolution is going downscale. These results do not confirm the allometric approach associated with a $V^{1/6}$ normalization.

DISCUSSION

The results obtained in the previous section can be understood from a more theoretical viewpoint by considering that each contribution to the voxel perfusion Q results from the contribution of each vascular segment input. It is thus proportional to the sum of the input flow coming from each input segment. When the vascular segment number is large, the total perfusion is then well approximated by the average flux per segment multiplied by the total number of segments. Since the voxel size is large (superior to 250^3 μm^3) compared with the vessel's spatial correlation length (estimated between 50 and 80 microns[12]), it can be considered that the surface vessel density is almost homogeneous along each voxel surface (because correlation length provides the scale above which the vessels random distribution can be considered as homogeneous for providing a sufficient statistical sampling). In this context, it is possible to approximate the number of input vessels by half the voxel surface times the vessel density (the other half being the total number of output vessels for which the blood leaves out flows outside the considered box). Since the total perfusion Q is proportional to the number of vessels, it is thus proportional to the voxel surface S, as confirmed by numerical simulations and Figure 2C. One might wonder whether this reasoning could lead to different consequences if, instead of using input arterial units, we chose the venular output ones, since their proportion is different (penetrating arteries represent 2/3 of all penetrating vessels[10]). Since inputs and outputs contribute to the same amount of total flux (a fact that we have explicitly checked in the numerical results), the weaker proportion of veins will be compensated by a larger average flux, and the proportionality of the total output perfusion flux with voxels surface is unchanged. Similarly, one could also question the fact that our results might be influenced by the undesirable contribution of the large penetrating vessels to the perfusion. Filtering the penetrating vessels contribution to the input flux leaves a similar surface rescaling to the CBF (not shown).

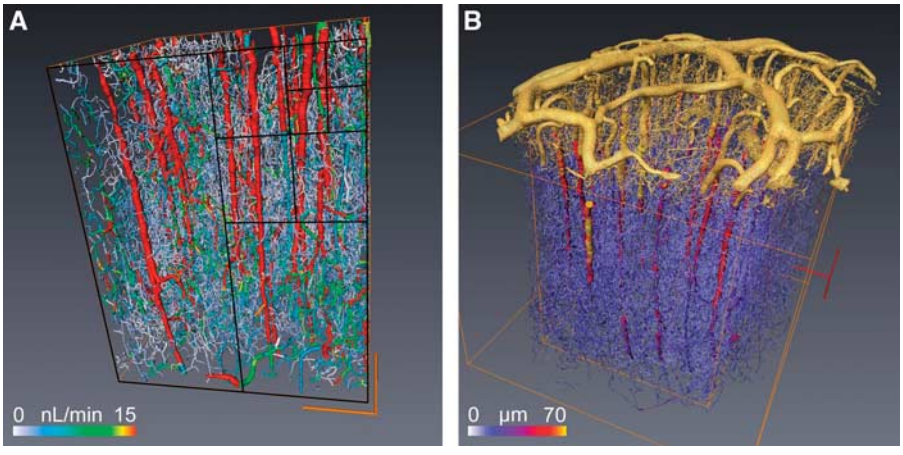

Figure 1. (**A**) The blood flow is computed for each vascular segment of the complete microvascular network in an 8-mm^3 volume of primate cortex, and color coded for blood flow values. The four sizes of boxes (250, 500, 1000, and 2000 microns) analyzed in Figure 2 are represented in the frontal face with black lines. The orange box represents the largest box. Box surface and volume are, respectively, noted as S and V. (**B**) This illustration shows the digitalized vascular structures of the pia matter in yellow connected with the intracortical vessels shown in (**A**) represented with a color range coding for the vessel diameter.

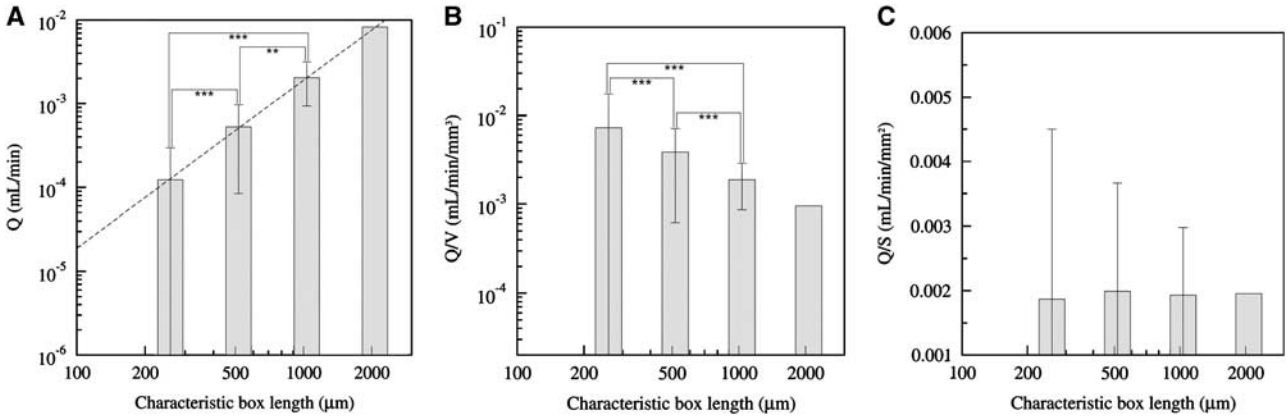

Figure 2. (**A**) Perfusion (incoming blood flow Q) computed for different box sizes in bilogarithmic representation. The dotted line is for surface variation (slope equals 2). (**B**, **C**) Different normalization scales for the blood perfusion Q versus the voxel box size: (**B**) Q/V versus the voxel-box length, (**C**) new surface normalization for the perfusion Q/S versus the voxel-box length. For (**A**, **B**) significant differences are indicated with asterisks: $***P<10^{-3}$ and $**P<5\times10^{-3}$, and for (**C**) $P>0.75$.

Furthermore, since we have only considered the influence of blood convection in our CBF evaluation, the role of supplementary diffusive processes on the proposed surface rescaling is questionable. Basic transport theory states that material transport goes as the flux times the area, implying that flux measurements should be normalized by the tissue area. Our findings thus highly suggest to consider a new reference parameter for brain perfusion that could be denoted as CBFs (s for surfacic CBF) which should scale as CBFs = CBF.V/S where V and S are the volume and the surface of the considered voxels. It is difficult to provide a convincing confirmation of this proposition from considering the available CBF data of the literature. First, because even though a large number of CBF measurements can be collected, voxel volume and surface values are rarely provided (even deduced from the acquisition set-up). Second, CBF values are found in various species (rabbit,[1] rat,[2] dog,[13] human,[3,14–21] and pig[22]) for various ages, sex, and brain regions, using various methods (CT, single-photon emission computed tomography, positron emission tomography, and magnetic resonance imaging). For low-resolution measurements, the possible joined contribution of gray and white matter could influence local CBF. Furthermore, the voxels are rarely cubic, and, most of the time, they are elongated parallelepiped (for which pial vessels might contribute). All these considerations could weaken the relevance of the proposed scaling for explaining the observed CBF variability when tested on the available data of the literature. Hence, our proposition should be challenged in the future using new dedicated measurements.

Finally, it is interesting to mention that the filtration velocity (or Darcy flux[23]), which is considered in porous media, is also a flow per surface unit (and not per volume unit) consistent with our finding for the brain perfusion. We hope that this work could improve CBF overall quality assessment and its validity domain, thus contributing to its better use in preclinical and clinical studies.

DISCLOSURE/CONFLICT OF INTEREST

The authors declare no conflict of interest.

ACKNOWLEDGEMENTS

The authors thank Pr A Steyer for interesting discussions.

REFERENCES

1 Cenic A, Nabavi DG, Craen RA, Gelb AW, Lee TY. Dynamic CT measurement of cerebral blood flow: A validation study. *AJNR Am J Neuroradiol* 1999; **20**: 63–73.
2 Adam JF, Elleaume H, Le Duc G, Corde S, Charvet AM, Troprès I *et al.* Absolute cerebral blood volume and blood flow measurements based on synchrotron radiation quantitative computed tomography. *J Cereb Blood Flow Metab* 2003; **23**: 499–512.
3 Ziegelitz D, Starck G, Mikkelsen IK, Tullberg M, Edsbagge M, Wikkelsö C *et al.* Absolute quantification of cerebral blood flow in neurologically normal volunteers: dynamic-susceptibility contrast MRI-perfusion compared with computed tomography (CT)-perfusion. *Magn Reson Med* 2009; **62**: 56–65.
4 Kudo K, Terae S, Katoh C, Oka M, Shiga T, Tamaki N *et al.* Quantitative cerebral blood flow measurement with dynamic perfusion CT using the vascular-pixel elimination method: comparison with H215O positron emission tomography. *AJNR Am J Neuroradiol* 2003; **24**: 419–426.
5 Gobbel GT, Cann CE, Fike JR. Measurement of regional cerebral blood flow using ultrafast computed tomography. Theoretical aspects. *Stroke* 1991; **22**: 768–771.
6 Karbowski J. Scaling of brain metabolism and blood flow in relation to capillary and neural scaling. *PLoS ONE* 2011; **6**: 26709–26721.
7 Plouraboué F, Cloetens P, Fonta C, Steyer A, Lauwers F, Marc-Vergnes JP. High resolution X-ray Imaging of vascular networks. *J Microsc* 2004; **215**: 139–148.
8 Risser L, Plouraboué F, Cloetens P, Fonta CA. 3D-investigation shows that angiogenesis in primate cerebral cortex mainly occurs at capillary level. *Int J Dev Neurosci* 2009; **27**: 185–196.
9 Risser L, Plouraboué F, Descombes X. Gap Filling of 3-D microvascular networks by tensor voting. *IEEE Trans Med Imaging* 2008; **27**: 674–687.
10 Guibert R, Fonta C, Plouraboué F. Cerebral blood flow modeling in primate cortex. *J Cereb Blood Flow Metab* 2010; **30**: 1860–1873.
11 Pries AR, Secomb T. Microvascular blood viscosity *in vivo* and the endothelial surface layer. *Am J Physiol* 2005; **289**: 2657–2664.
12 Risser L, Plouraboué F, Steyer A, Cloetens P, Le Duc G, Fonta C. From homogeneous to fractal normal and tumorous microvascular networks in the brain. *J Cereb Blood Flow Metab* 2007; **27**: 293–303.
13 Gobbel G, Cann C, Iwamoto H, Fike J. Measurement of regional cerebral blood flow in the dog using ultrafast computed tomography. Experimental validation. *Stroke* 1991b; **22**: 772–779.
14 Takeuchi R, Yonekura Y, Matsuda H, Konishi J. Usefulness of a three-dimensional stereotaxic ROI template on anatomically standardised 99mTc-ECD SPET. *Eur J Nucl Med* 2002; **29**: 331–341.
15 Qiu D, Staka M, Zun Z, Bammer R, Moseley M, Zaharchuk G. CBF measurements using multidelay pseudocontinuous and velocity-selective arterial spin labeling in patients with long arterial transit delays: Comparison with xenon CT CBF. *J Magn Reson Imaging* 2012; **36**: 110–119.
16 Zaharchuk G, Straka M, Marks MP, Albers GW, Moseley ME, Bammer R. Combined arterial spin label and dynamic susceptibility contrast measurement of cerebral blood flow. *Magn Reson Med* 2010; **63**: 1548–1556.
17 Xyda A, Haberland U, Klotz E, Bock HC, Jung K, Knauth M *et al.* Brain volume perfusion CT performed with 128-detector row CT system in patients with cerebral gliomas: a feasibility study. *Eur Radiol* 2011; **21**: 1811–1819.

18 Grandin CB, Bol A, Smith AM, Michel C, Cosnard G. Absolute CBF and CBV measurements by MRI bolus tracking before and after acetazolamide challenge: Repeatability and comparison with PET in humans. *Neuroimage* 2005; **26**: 525–535.
19 Astergaard L, Johannsen P, Hbst-Poulsen P, Vestergaard-Poulsen P, Asboe H, Gee AD *et al*. Cerebral blood flow measurements by magnetic resonance imaging bolus tracking: comparison with [15O]H2O positron emission tomography in humans. *J Cereb Blood Flow Metab* 1998; **18**: 935–940.
20 Astergaard L, Smith DF, Vestergaard-Poulsen P, Hansen SB, Gee AD, Gjedde A *et al*. Absolute cerebral blood flow and volume measured by magnetic resonance imaging bolus tracking: comparison with positron emission tomography values. *J Cereb Blood Flow Metab* 1998; **18**: 425–432.
21 Smith AM, Grandin CB, Duprez T, Mataigne F, Cosnard G. Whole brain quantitative CBF and CBV measurements using MRI bolus tracking: comparison of methodologies. *Magn Reson Med* 2000; **43**: 559–564.
22 Sakoh M, Rohl L, Gyldensted C, Gjedde A, Astergaard L. Cerebral blood flow and blood volume measured by magnetic resonance imaging bolus tracking after acute stroke in pigs: comparison with [O]-H2O positron emission tomography. *Stroke* 2000; **31**: 1958–1964.
23 Bear J. *Dynamics of Fluids in Porous Media*. American Elsevier Publishing Company: New York, NY, USA, 1972.